

Molecular Structure of the Chloroform–Water and Dichloromethane–Water Interfaces[†]

Dennis K. Hore,[‡] Dave S. Walker, Libby MacKinnon,[§] and Geraldine L. Richmond^{*}

Department of Chemistry, University of Oregon, Eugene, Oregon 97403

Received: October 31, 2006; In Final Form: December 19, 2006

Using equilibrium molecular dynamics simulations, we investigate the structure of chloroform–water and dichloromethane–water interfaces. These systems are analyzed in terms of the orientation of water, chloroform, and dichloromethane molecules as a function of distance from the Gibbs surface. We also calculate order parameters for all molecules across the interface. The results show that the structures may be described in the context of a few distinct regions of the interface, where organic and water molecules generally arrange themselves either to maximize hydrogen-bonding interactions or to minimize the net dipole moment. In cases where molecular arrangements promote hydrogen-bonding interactions, they often do not provide complete dipole compensation. The orientation of organic and water molecules then creates a field across the interface. For the CHCl_3 –water interface, the field has a uniform direction with the positive end of the dipole pointing toward the bulk water phase. The interfacial field is more complicated in the case of CH_2Cl_2 –water but is oriented in the same direction close to the bulk water side.

1. Introduction

The interface between water and chlorinated organic liquids is of central importance to a broad category of scientific, industrial, biological, and environmental disciplines. Chloroform and dichloromethane (DCM) in particular have received a lot of attention, primarily because of their widespread use as solvents but also because the small size of these molecules is amenable to computational study. Because chloroform is often considered a model hydrophobic polar liquid, there have been many experimental and simulation studies of molecules adsorbed at the chloroform–water interface. These include ions of various sizes,^{1,2} proteins,^{4,5} phospholipids,⁷ nanocrystals,⁸ polymer–enzyme complexes,^{9,10} and polyelectrolytes.⁷ Given this wide range of applications, it is surprising that there have not been more studies of the neat chloroform–water interface, with the exception of early interfacial tension measurements^{11,12} and studies of chloroform adsorbed to ice.^{13,14} The dichloromethane–water interface has a similar spectrum of applications, such as self-assembly of polymer surfactants,^{16–18} solvent dechlorination,²⁰ ion partitioning,²¹ and microemulsions of these two liquids.^{22,23} There is also biological interest in this liquid–liquid interface with studies of adsorbed phospholipids²⁴ and proteins.^{25–28} The neat dichloromethane–water interface has been studied by means of interfacial tension measurements³⁰ and molecular dynamics simulation.³¹ In nearly all of the above studies where structural information is sought, it is either of a surfactant at the liquid–liquid interface or of the water molecules. This paper addresses the interfacial structure by examining the mutual orientation of the water and organic molecules as a function of depth through the interface.

The nature of the charge at a liquid interface is an important consideration, both from a fundamental standpoint and as an

important contributor to surfactant structure. At biological interfaces, for example, the structure of many proteins is stabilized by association with solvated ions. The historic opinion has been that ions are repelled from the interface between water and a hydrophobic medium.^{32,33} This view has been challenged recently with detailed molecular dynamics studies that show an enhancement of polarizable anions at the air–water interface,^{35,36} and this provides some justification for the observed negative charge at many hydrophobic interfaces with water.³⁷ It has been demonstrated recently that the origin of this effect may lie in a field created by oriented interfacial water molecules.³⁸ This field would then attract hydroxide ions, either from the autodissociation of water or from an additional source, to the interface. The current study entails detailed investigations of the orientation of both water and organic molecules at the interface. We will therefore use our findings on the structure to additionally speculate on the origin, size, and polarity of any orientation-induced field at the interface and discuss its consequence on the surface charge.

We will begin with a brief overview of the details of our molecular dynamics simulations, followed by a description of the primary analyses performed with the resulting data. Two systems will then be discussed in turn, starting with the chloroform–water interface, followed by the dichloromethane–water interface. A general comparison of these two systems then follows.

2. Simulation Details

Equilibrium molecular dynamics simulations were performed with the Amber 7 package³⁹ (using the Amber 7 force field) and an integration time of 1 fs. Initial configurations consisted of separate (40 Å)³ boxes, each containing 2135 POL3³⁹ water, 475 chloroform, or 601 dichloromethane molecules. These were subject to energy minimization and were then equilibrated for 200 ps. Temperature was controlled by weak coupling to a heat bath at 300 K; molecular geometries were constrained using the SHAKE algorithm; long-range interactions were cut off at 8 Å using the Particle Mesh Ewald technique. The partial atomic

[†] Part of the special issue “Kenneth B. Eisenthal Festschrift”.

^{*} Corresponding author. E-mail: richmond@uoregon.edu. Phone: 541-346-4635. Fax: 541-346-5859.

[‡] Present address: Department of Chemistry, University of Victoria, Victoria, British Columbia, V8W 3V6, Canada.

[§] Department of Chemistry, California Polytechnic State University, San Luis Obispo, CA 93407.

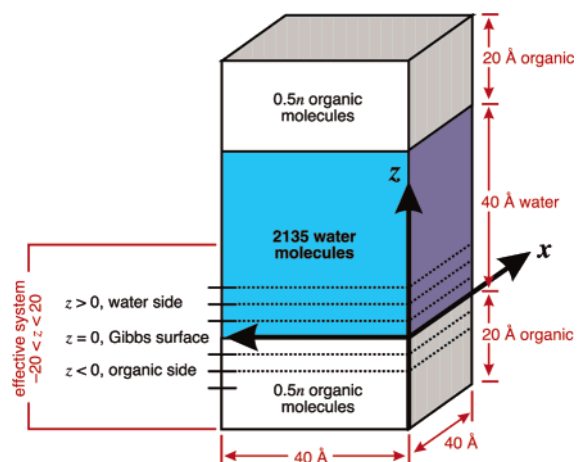


Figure 1. Organic and water boxes, showing the configuration of the system for molecular dynamics simulations. Values of n depend on the density of the organic liquid. $z = 0$ corresponds to the lower Gibbs surface. For all analyses, molecules above the system center are treated as if they originated in a corresponding location in the lower half of the box. The dotted lines depict 1-Å-thick slabs that were used to obtain the statistics for the analyses.

charges that were used to construct the organic models were used from the Amber 7 library for chloroform (same as Dang's polarizable model⁴⁰) and from the literature for dichloromethane.⁴¹ Water–organic boxes were then assembled as illustrated in Figure 1. Such configurations allowed for easier control of the center of mass while instituting periodic boundary conditions in all three directions. The energy of the entire system was then minimized and allowed to reach equilibrium by following the dynamics for 2 ns. Snapshots of all of the coordinates were then recorded every 50 fs for 10 ns, thereby collecting 200 000 configurations. It was necessary to collect such a large amount of data (nearly 1 Tb of files on disk) because the sought information on the molecular orientation would be obtained through the generation and analysis of joint tilt–twist angle histograms. It has been recognized that constructing such plots with useful resolution typically requires about an order of magnitude more data than would be used for one-dimensional analyses.^{42,43} All calculations and analyses were performed on our 16-processor AthlonMP/Opteron cluster, running Fedora Core 3 linux, and using the LAM message-passing libraries.

3. Results

We now examine all of the data produced by the molecular dynamics simulations to arrive at a structural description of the interface between water and the two chlorinated organic liquids. First, we will describe the two categories of quantities that we have calculated, namely, order parameters and orientation histograms. Next, we will outline the results of each system in turn, beginning with the chloroform–water interface. For each system, we will first show the order parameters for water and the organic species to gain a qualitative understanding of interfacial features. This will be followed with an analysis of the orientation histograms to arrive at a detailed picture of the water and organic structure. This data will then be summarized with structural diagrams to illustrate the orientation of both species throughout the interface. Finally, we use knowledge of this orientation to comment on the dipolar interactions between water and organic species to generate net fields perpendicular to the plane of the interface.

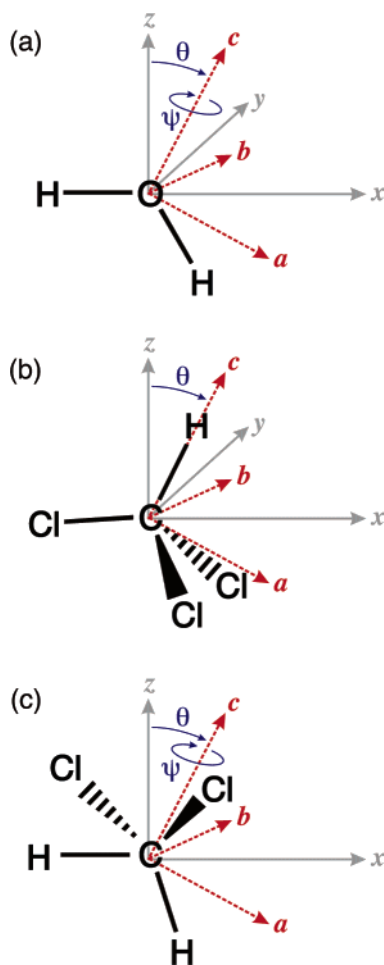


Figure 2. In the laboratory frame, the Gibbs dividing surface is in the xy plane, so z is the normal to this plane. (a) In the frame of the water molecule, c is defined to be along the C_2 symmetry axis, pointing away from the hydrogens. The molecule lies in the ac plane. The Euler angle, θ , is defined as the angle between the z and c unit vectors. The twist angle, ψ , parametrizes the rotation about the molecular c axis. (b) For chloroform, the C–H vector defines the molecular c axis. (c) The dichloromethane axes are defined in an analogous manner to those of the water molecule, with H–C–H defining the ac plane, and the c axis bisecting the H–C–H angle.

3.1. Quantitative Description of Molecular Orientation.

There are two useful metrics for describing the orientation of molecules at a liquid interface. One is the extent to which the collection of molecules is ordered with respect to a designated direction in the laboratory frame; the other is the actual orientation of the molecules, specified by Euler angles (θ , ϕ , ψ) that relate the molecule-fixed to laboratory frames. The first description is achieved by specifying three biaxial order parameters.^{44–46} One is for the tilt angle, θ , defined as the angle between the molecular c axis and the interface normal, z . (The relevant molecular frame axes for each molecule are defined in Figure 2.)

This order parameter is

$$S_1 = \frac{1}{2} \langle 3 \cos^2 \theta - 1 \rangle. \quad (1)$$

For chloroform, we will assume that there is very weak (if any) orientational preference for rotation about the C–H axis, so S_1 will completely describe the order. For water and dichloromethane, however, we must consider that a twist preference about the molecular c axis may be significant. For those systems,

we therefore additionally determine a twist (ψ) order parameter

$$S_2 = \frac{\langle \sin \theta \cos 2\psi \rangle}{\langle \sin \theta \rangle}. \quad (2)$$

A three-dimensional orientation normally requires the additional specification of an azimuthal (ϕ) orientation, and corresponding order parameter S_3 . In the case of a liquid, however, there can be no anisotropy about the surface normal, so $S_3 = 0$ for all molecules in the bulk and throughout the interface. The ranges for these order parameters are $-0.5 < S_1 < 1$ and $-1 < S_2 < 1$. $S_1 = 1$ indicates that all molecules are perfectly aligned with their C_2 axes parallel (or antiparallel) to the interface normal; $S_1 = -0.5$ indicates that they are perfectly aligned perpendicular to the interface normal, with their symmetry axes in the plane of the interface. Likewise, for S_2 a value of 1 indicates complete alignment of all molecules with $\psi = 0^\circ$ or 180° ; a value of -1 indicates that the corresponding angle is 90° or 270° . An isotropic distribution would have all order parameters equal to zero.

Although the order parameters provide an insightful description of the extent of the molecular orientation at various depths, z , with respect to the Gibbs surface (GS, $z = 0 \text{ \AA}$), they do not suffice to describe the actual orientation of the molecules. To study this orientation directly, we constructed joint tilt–twist θ – ψ angular histograms for 20 1- \AA -thick slabs ranging from $z = -11 \text{ \AA}$ (on the bulk organic side of the GS) to $z = +8 \text{ \AA}$ (on the bulk water side). The ranges of the Euler angles in the current definition are $0^\circ \leq \theta \leq 180^\circ$ and $0^\circ \leq \psi \leq 360^\circ$. As a result of the molecular symmetry (C_{2v} for water and dichloromethane; $C_{\infty v}$ for chloroform's C–H bond) and the isotropic distribution in the azimuthal angle ϕ , the twist angle is unique only in the range $0^\circ \leq \psi \leq 90^\circ$. We have chosen to plot $0^\circ \leq \psi \leq 180^\circ$ and so this symmetry is apparent. Because the data is noisy in regions where there are few molecules (water molecules in the organic phase, or organic molecules in the water phase), this repeated range for ψ allows for an easy visual discrimination of noise artifacts from real trends.

Even with a sample size that consists of 200 000 configurations of the entire system, the resulting histograms had a fair amount of noise. We have resolved this issue by applying a 15×15 pixel (degree) median filter. Median filtering is very common in data⁴⁸ and image⁴⁹ analysis. It generally does a better job than a Gaussian filter and has two primary advantages over a simple mean filter. First, the median is more robust than the mean because it is not as sensitive to outliers. Second, because the median value is indeed one of the histogram values, no new counts are created in the histogram images. We have verified that in all cases the median filtering does not alter the location, relative intensity, or shape of the features. The detailed features of the results for each system will now be described in turn.

3.2. Chloroform–Water Interface. Tilt and twist order parameters for the chloroform–water interface are shown in Figure 3. Classifying the interfacial structure according to the sign of the order parameters results in three regions. In the first one, labeled A in Figure 3, S_1 and $S_2 > 0$ for water and $S_1 \approx 0$ for chloroform. This indicates that water molecules are aligned such that their symmetry axes are closer to the interface normal than to the plane of the interface, and there is negligible orientation of the chloroform here. In regions B and C, $S_1 < 0$ for water and $S_1 > 0$ for chloroform. In this region, water molecules have their symmetry axes aligned parallel to the plane of the interface. The chloroform C–H vector is aligned along the interface normal. With this water axis orientation, we still need to distinguish between straddling molecules (with one O–H bond

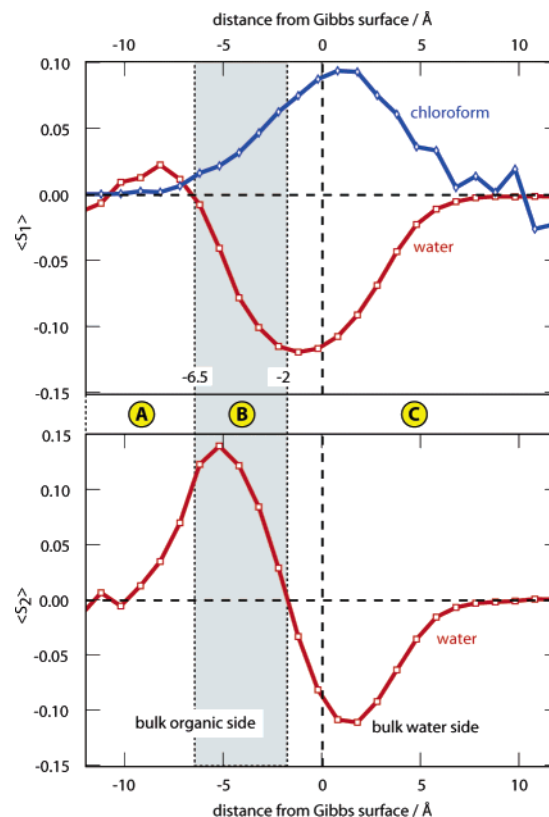


Figure 3. Tilt S_1 and twist S_2 order parameters for water (red) and chloroform (blue) at the chloroform–water interface. The behavior of both molecules throughout the interface may be grouped into three distinct regions (A–C), described in the text.

directed toward the bulk water phase, and the other O–H bond toward the bulk chloroform) and in-plane molecules (with the H–O–H plane parallel to the Gibbs surface). Straddling water appears as $S_2 > 0$ (region B) and in-plane water appears as $S_2 < 0$ (region C) in the bottom part of Figure 3.

A more complete description of the orientation requires studying the orientation histograms shown for water in Figure 4 and chloroform in Figure 6. For water, these are shown as joint θ – ψ histograms assembled at 1 \AA slices through the interface. Bold inset numbers indicate distance (in angstroms) from the Gibbs dividing surface, located at $z = 0 \text{ \AA}$. The bulk chloroform phase occurs at $z < 0 \text{ \AA}$; the bulk water phase at $z > 0 \text{ \AA}$. Blue colors indicate low populations, and red colors indicate large populations, relative to that of an isotropic distribution of molecules (such as found in the bulk water phase). The slices in the top row ($z = -11$ to -8 \AA) appear uniformly blue because there are few water molecules this deep in the chloroform, and they do not have any preferred orientation with respect to the surface. Likewise, the slices in the bottom row ($z = 5$ – 8 \AA) are red because there are many water molecules on the bulk water side of the interface. The last slice ($z = 8 \text{ \AA}$) has a near-uniform intensity, indicating that the water molecules have no preferred orientation this far from the interface. Beginning at $z = -6 \text{ \AA}$ (region A) on the chloroform side of the interface, a bright stripe along $\theta = 0^\circ$ is present, evidence for water aligned with its symmetry axis along the interface normal. Additionally, these histograms reveal the “sense” of this orientation: the water molecules here have their oxygens pointing toward the bulk water phase, and hydrogens toward the bulk chloroform. A typical slice in the center of region B may be seen at $z = -4 \text{ \AA}$, where the distribution of water symmetry axes is centered at $\theta = 70^\circ$ from the interface normal, and the

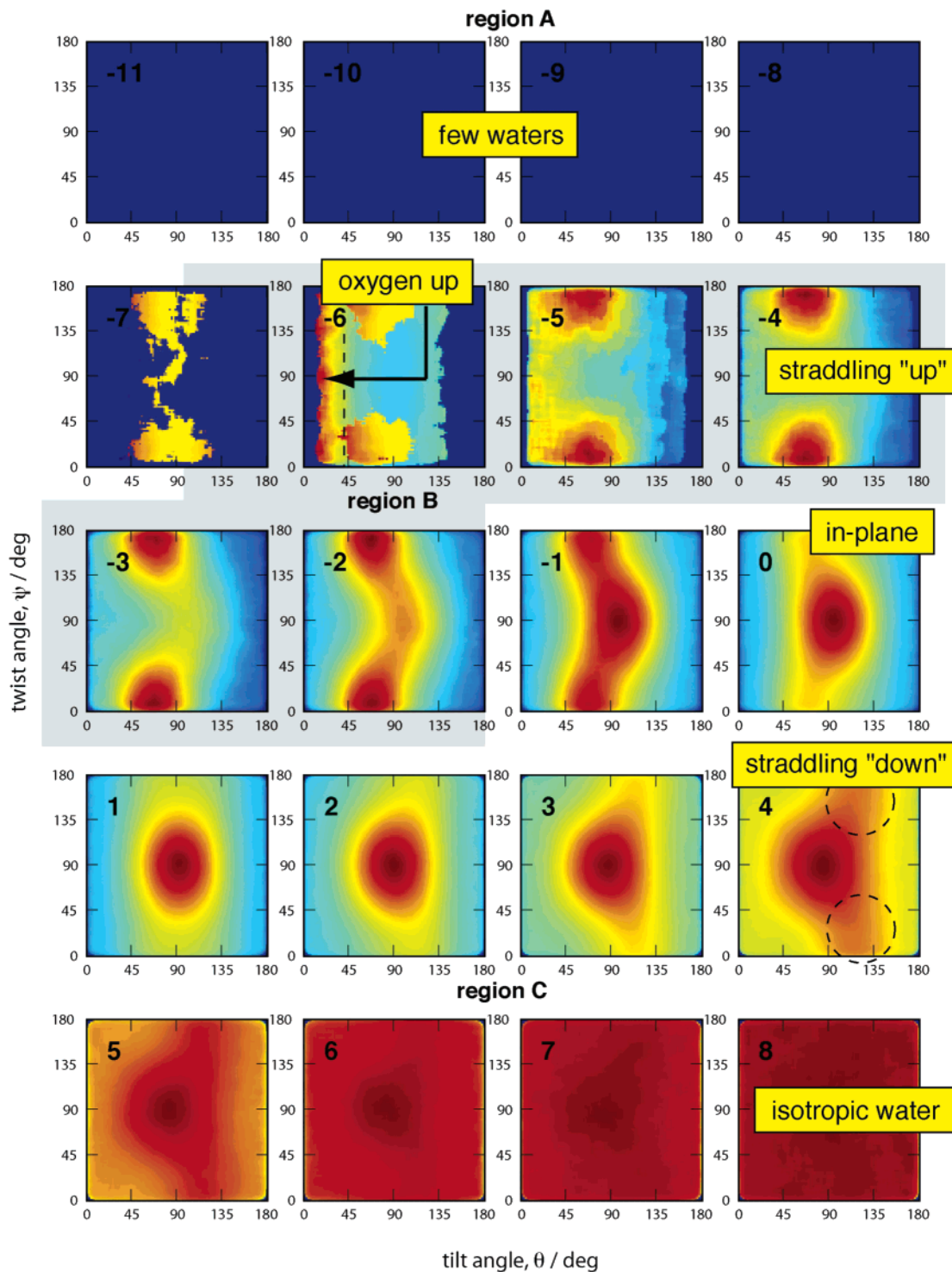


Figure 4. Snapshots of water molecule orientation at the chloroform–water interface. Blue indicates the smallest population; red indicates the largest population. Bold inset numbers indicate distance (in angstroms) from the Gibbs dividing surface. Negative values are on the bulk organic side; positive values are on the bulk water side. Shaded gray background is used to distinguish regions A–C, classified according to the order parameters in Figure 3.

twist angle distribution is centered at $\psi = 0, 180^\circ$, indicative of straddling water molecules with one O–H bond directed toward the chloroform and the other toward the bulk water. This geometry is illustrated in Figure 5a and results in a fairly narrow angular distribution for the OH oscillator directed toward the organic phase (the so-called “free OH”) centered at 18° from the interface normal. The transition region between dominant straddling and in-plane orientations observed as $S_2 = 0$ at $z \approx -1.5 \text{ \AA}$ may be studied in the $z = -2 \text{ \AA}$ and $z = -1 \text{ \AA}$ slices of Figure 4. Between these distances, we can see an equal

preference for both orientations. The histogram at $z = +2 \text{ \AA}$ is representative of strongly oriented water molecules in region C. Here we can see that the orientation distribution is centered about $\theta = 90^\circ, \psi = 90^\circ$ describing in-plane water molecules (Figure 5b). A fine feature in these histograms, not observed in the order parameters, is the onset of a second straddling distribution at $z > 1 \text{ \AA}$. However, unlike the one that comprises the major water orientation on the organic side of the GS (labeled “up”), this one has the water symmetry axis tipped downward to $\theta = 120^\circ$. This species (illustrated in Figure 5c,

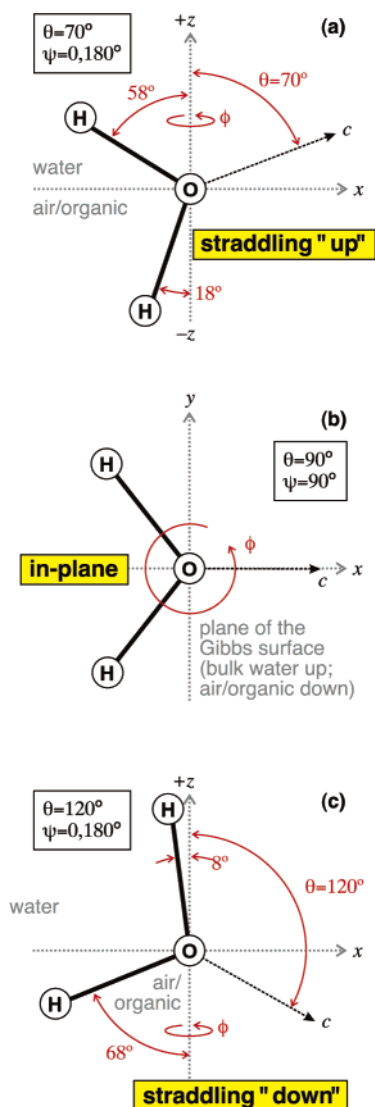


Figure 5. Dominant orientations of water molecules at the chloroform–water interface. (a) Deepest into the organic phase (regions A and B), straddling water molecules have their symmetry axes tilted upward, toward the bulk water. (b) Moving past the GS toward the bulk water phase, the dominant orientation in region C becomes in-plane water molecules. (Note that the axes in this frame are x and y .) (c) Coexisting with in-plane water molecules in region C, there is a lesser population of straddling species. Here the symmetry axes are tipped away from the bulk water phase. Azimuthal rotation ϕ is indicated as a reminder that the orientation is uniformly distributed about z .

labeled “down”) has a broad distribution of free OH angles centered at 68° from the interface normal.

The chloroform orientation distribution may be described in a more compact manner in Figure 6 because we are tracking only the tilt angle of the C–H bond. We can see that the strong alignment of this bond parallel to the interface normal has a polarity such that the hydrogen points toward the bulk water phase. The orientation distribution has a peak between 0° and 20° from the interface normal, a width (at half max) of about 10 \AA , centered around 2 \AA into the bulk water phase. Greater than ca. 6 \AA into the bulk water phase, the histogram appears noisy because there are so few chloroform molecules in this region.

Considering the water and organic orientations together, it is evident that the maximum extent of chloroform orientation (seen as the peak of the blue chloroform curve, 2 \AA into the bulk water phase in the top part of Figure 3) coincides with the

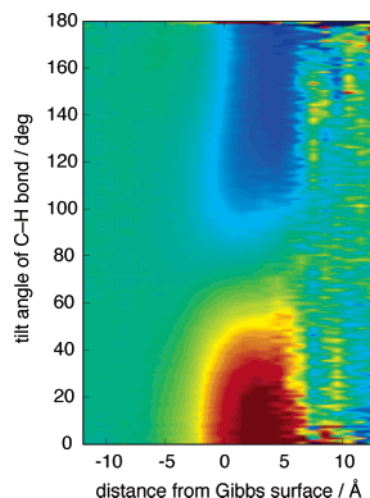


Figure 6. Orientation distribution of the chloroform C–H axis, additionally binned according to distance from the Gibbs surface. Blue colors indicate small population; red colors indicate large population of chloroform relative to the bulk isotropic distribution.

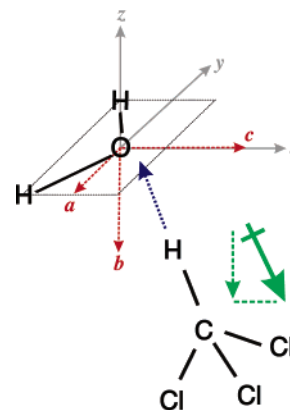


Figure 7. Hydrogen-bonding geometry corresponding to the maximum orientation of chloroform molecules. Dashed blue arrows indicate hydrogen bonds between water and chloroform; green arrows show the direction of the chloroform permanent dipole moment.

maximum extent of in-plane water molecule orientation (negative peak of $S_2 < 0$ for water in the bottom part of Figure 3). Figure 7 shows that this arrangement is optimal for hydrogen bonding between water and chloroform. This may also account for the reason that the distribution of C–H bond vectors are not more tightly constrained about the interface normal: a tilt of the C–H bond creates a stronger H bond with in-plane water molecules. Water molecules in this orientation have their permanent dipoles in the plane of the interface. For the chloroform molecules, however, there is an out-of-plane component of the permanent dipole moment, indicated by the green arrows in Figure 7.

Now that we have a quantitative understanding of the orientation of water and chloroform molecules throughout the interface, it is interesting to consider the combined effect of number density and orientation on the field across the interface. Figure 8 shows the projection of the permanent dipole moment for the water (red) and chloroform (blue) molecules across the interface. The total out-of-plane dipole moment (water and chloroform together) is plotted in black. In our convention, dipoles oriented such that their positive end (“plus” side of the arrow in the figure) is directed up toward the bulk water are assigned positive values of the polarization on the y axis. If the negative end of the dipole (arrowhead) is oriented in this direction, then the polarization is given a negative sign. On the

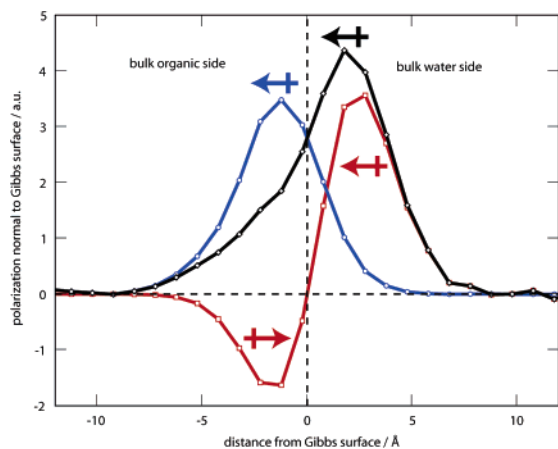


Figure 8. The z -component of the net dipole moment for 1 Å slabs through the chloroform–water interface. Contributions from water molecules are shown in red, chloroform in blue, total out-of-plane dipole moment in black. The sign of the polarization indicates the direction of the net dipole moment, depicted with arrows.

basis of what we have seen in our orientation analysis, it is no surprise that water molecules on the organic side of the interface contribute to setting up a field that is negative toward the bulk water and positive toward the bulk organic. This results from the water dipole axes being, on average, tilted slightly up so the more electronegative oxygens are directed toward the bulk water phase (Figure 5a). On the bulk water side of the Gibbs surface, however, the dominant orientation for water molecules is their dipolar axes in the plane of the surface. We have, however, described a smaller population that is also straddling the interface here, but with its dipolar axes tipped toward the bulk organic phase (Figure 5c). It is these molecules that create a field with the opposite polarity (positive in our convention). We have seen that the chloroform molecules are pointed in the same direction throughout the region in which they are oriented. This creates a field with the same sign as that from the water molecules on the bulk water side of the GS. In the region where the water polarization is negative, the positive chloroform polarization has a greater magnitude. As a result, the overall net dipole moment is oriented such that the negative end is on the bulk organic side of the interface and the positive end is on the bulk water side.

3.3. Dichloromethane–Water Interface. We will investigate the structure of the dichloromethane–water interface using the same treatment we applied to the chloroform water interface. As an overview, tilt and twist order parameters for the DCM–water interface are shown in Figure 9. The behavior of these molecules is slightly more complicated than that for the chloroform water interface, and so the analyses will be categorized in terms of four regions, labeled A–D. The actual orientation of the water molecules will be shown in the joint θ – ψ histograms in Figure 10. Again, the same general features observed for the chloroform–water interface will be identified here, but the appearance of the data is quite different on account of the more pronounced oxygen-up water orientation, to be described below. Because the orientation of dichloromethane molecules also necessitates the specification of tilt and twist angles, this will be described by additional θ – ψ histograms in Figure 12. We now describe features of the DCM–water interface, moving from the layers deepest in the organic phase (region A) toward the bulk water side of the interface (region D).

Examining the order parameters in Figure 9 shows that in region A, S_1 and $S_2 > 0$ for water; $S_1 > 0$ and $S_2 < 0$ for dichloromethane. Together with an inspection of the joint θ – ψ

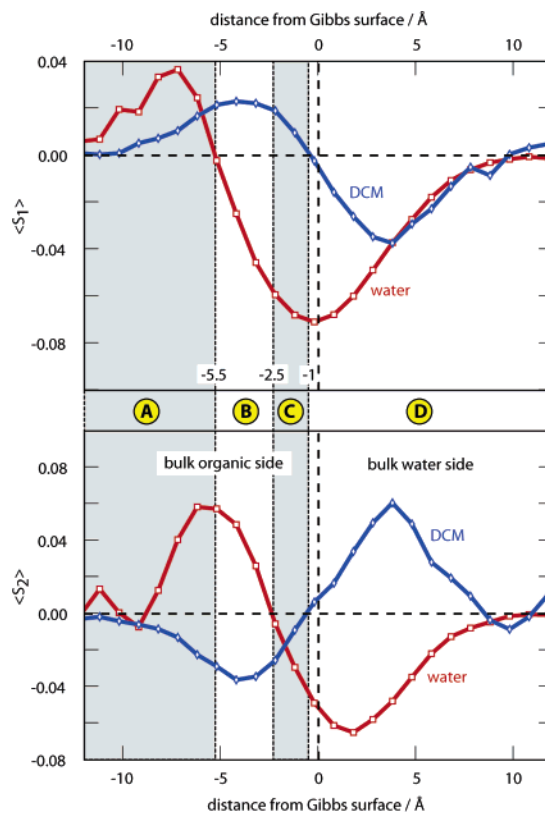


Figure 9. Tilt S_1 and twist S_2 order parameters for water (red) and dichloromethane (blue) at the dichloromethane–water interface. The behavior of both molecules throughout the interface may be grouped into four distinct regions (A–D), described in the text.

histograms for water (Figure 10) and dichloromethane (Figure 12), we can conclude that both molecules are generally oriented with their molecular c axes (defined in Figure 2) pointing toward the bulk water phase. This same feature was observed for the chloroform–water interface, but the extent of the orientation is much greater for dichloromethane as evidenced by the magnitude of the order parameter and the orientation profiles in the histograms. Figure 13a illustrates this orientation and shows that water and DCM molecules are arranged to maximize their hydrogen-bonding interactions. It is interesting to note, however, that this arrangement does not offer any cancellation of the permanent dipole moments of either molecule. We should therefore expect a large interfacial field on the organic side of the Gibbs surface. A close examination of the organic orientation histograms in Figure 12 reveals a second, minor population of DCM molecules that have their chlorine atoms pointing toward the bulk organic phase and hydrogen atoms pointing up toward the bulk water phase. Figure 13b illustrates that this does not create any H-bonding opportunities with water molecules in the same region. Even water molecules in higher layers (closer to the Gibbs surface) will not H-bond favorably with such DCM orientations because those also have their oxygens pointing up toward the bulk water. However, the dipole arrows in Figure 13b show that the motivation for this arrangement may in fact be compensation of the water and organic permanent dipole moments.

In region B, which occurs between $z = -5.5$ Å and -2.5 Å, $S_1 < 0$ and $S_2 > 0$ for water while $S_1 > 0$ and $S_2 > 0$ for dichloromethane. This region contains straddling water molecules, with their H–O–H plane perpendicular to the plane of the Gibbs surface. There is a gradual change from the oxygen-up orientation (shown in Figure 11a) of the previous layers to the straddling orientations observed here. During this progres-

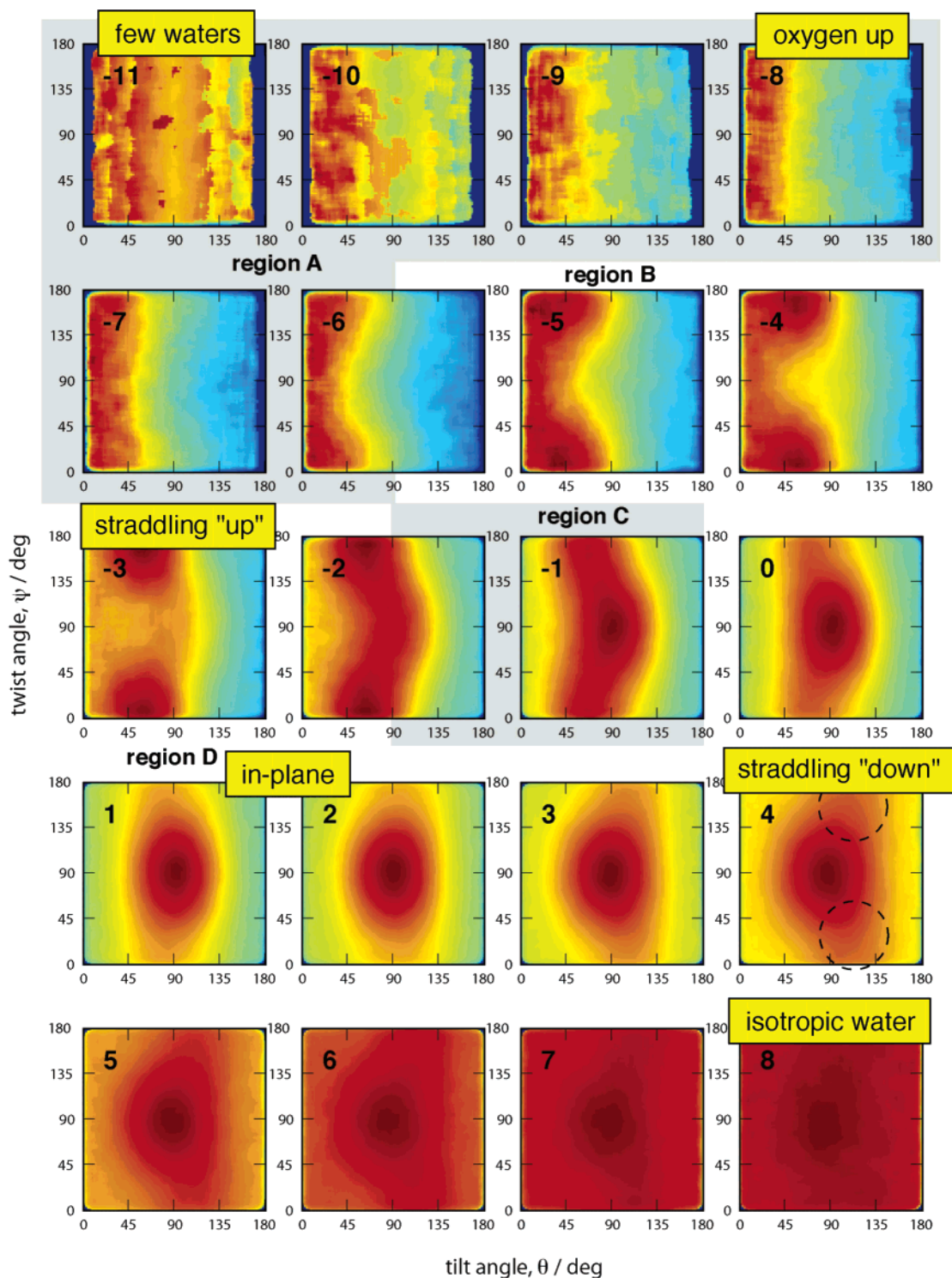


Figure 10. Snapshots of water molecule orientation at the dichloromethane–water interface. Blue indicates the smallest population; red indicates the largest population. Bold inset numbers indicate distance (in angstroms) from the Gibbs dividing surface. Negative values are on the bulk organic side; positive values are on the bulk water side. Shaded gray background is used to distinguish regions A–D, classified according to the order parameters in Figure 9.

sion, the tilt angle of the water symmetry axis increases from 37° at $z = -5 \text{ \AA}$ (free OH centered at 15° ; Figure 11b) to 58° at $z = -3 \text{ \AA}$ (free OH centered at 6° ; Figure 11c) to 63° at $z = -2 \text{ \AA}$ (free OH centered at 11° ; Figure 11d). As a result of the azimuthal isotropy, these angles describe cones about the interface normal. Looking at the organic orientation for the corresponding slices in Figure 12 shows that there are now two populations of dichloromethane. The dominant one is oriented as it was in region A, with chlorine atoms pointing up toward the bulk water phase. There is now an additional small

population of organic molecules that have their hydrogen atoms in the plane of the interface and their chlorine atoms straddling this plane.

In region C, the small distance between $z = -2.5 \text{ \AA}$ and $z = -1 \text{ \AA}$, dichloromethane molecules are oriented as in the previous region, only to a lesser degree. The water molecules, however, have begun to make their transition to an in-plane orientation. At this point, both straddling and in-plane orientations of water molecules have nearly equal populations, as can be seen between the -2 \AA and -1 \AA slices in Figure 10. In this region, an

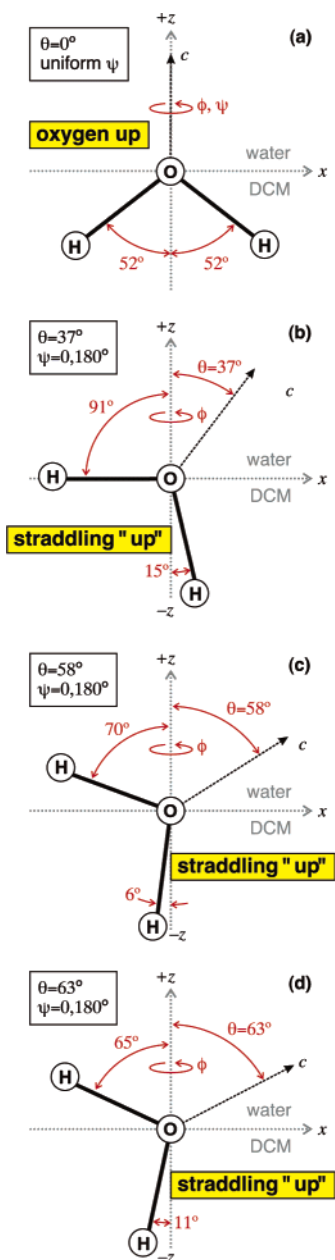


Figure 11. Orientation of water molecules on the organic side of the GS for the dichloromethane–water interface. (a) Deepest into the organic layer in region A, water molecules are aligned with their symmetry axes normal to the GS. By definition, this necessitates the twist angles being uniformly distributed (ψ and ϕ are degenerate here). (b–d) Moving toward the GS in region B, the symmetry axes of the straddling “up” water molecules become closer to the plane of interface. (In-plane and straddling “down” molecules in regions C and D are not illustrated and have orientations similar to those shown in Figure 5.)

interesting subpopulation of DCM molecules develops, with the Cl–C–Cl plane tilted approximately 120° from the interface normal. Figure 13c shows that such an orientation of DCM molecules may favorably H bond with the emerging in-plane orientation of water. Figure 13c also illustrates that the diminishing straddling water molecules in this region (tilted at 120°) are not able to make strong H-bonds to DCM in this orientation. However, these organic and straddling water molecules have components of their permanent dipole moments that cancel each other within this region of the interface.

Finally in region D of Figure 9 ($-1 \text{ \AA} < z < 12 \text{ \AA}$), water molecules exhibit S_1 and $S_2 < 0$, while dichloromethane

molecules show $S_1 < 0$ and $S_2 > 0$. The corresponding histograms in Figures 10 and 12 show that this is to be interpreted in terms of in-plane water molecules and organics with their hydrogens straddling the plane (chlorine atoms in the plane of the Gibbs surface). Figure 13d illustrates that this arrangement is motivated by good hydrogen-bonding geometry. Because the permanent dipole moments of both species are largely in the plane of the interface, we should not expect a large overall out-of-plane dipole moment for this region of the interface.

With the above knowledge of the water and dichloromethane orientations, we now consider the net dipole moment across the dichloromethane–water interface. Figure 14 shows the out-of-plane dipole moment of water (red), dichloromethane (blue), and the combined total (black). The water polarization profile has the same general shape as it did for the chloroform–water interface, but here the negative region on the organic side of the interface has about three times the magnitude of the positive region on the bulk water side. The DCM polarization is negative throughout the interfacial region and makes a very small contribution to the total dipole moment on the bulk water side of the interface. Overall, the net dipole changes sign through the interface, with positive ends oriented in the direction of both bulk phases, and a negative region localized about 2 \AA into the bulk water phase. The area under the net dipole moment curve (black in Figure 14) that also corresponds to regions with significant bulk water concentration are filled with a gray hatch pattern. It may be noticed that the positive and negative hatched regions are nearly equal in area, additionally minimizing the net field in the water region of the interface.

4. Discussion

There have been many detailed structural investigations from simulations of the neat air–water interface^{50–52} and the interface between water and other organic liquids such as carbon tetrachloride,^{54,43} dichloromethane,³¹ dichloroethane,⁵⁶ and benzene.⁵⁷ Of particular relevance to the current study is the detailed water structure at a variety of interfaces investigated by joint tilt–twist histograms by Jedlovsky et al.^{42,43} The authors have used slices through the interfacial region to identify straddling water molecules near the organic side of the Gibbs surface and in-plane water molecules near the bulk water side. Because of the small size of their system and short simulations, however, this was the extent of the detail that could be extracted from their orientation histograms, an important contribution at the time. In the current study, the statistics afforded by a large number of molecules, large area of the interface, and length of the simulations enabled high-resolution maps of the orientation of both water and organic molecules. For the water structure, there are two primary additional features that can therefore be observed in our data. The first is the preference of the straddling water population on the organic side of the GS to point its symmetry axis toward the bulk water phase. The second is the identification of a second straddling water population, on the water side of the GS, coexisting with the dominant in-plane orientation in that region, and with their symmetry axes pointing toward the bulk organic side of the interface. The important consequence of these water molecules, observed in both the chloroform–water and DCM–water systems, is that they result in a net water dipole component normal to the interface, with negative charge pointing toward the GS on the organic side and negative charge pointing away from the GS on the water side. Had this subset of straddling water molecules on the water side not been observed, it would have been difficult to account for

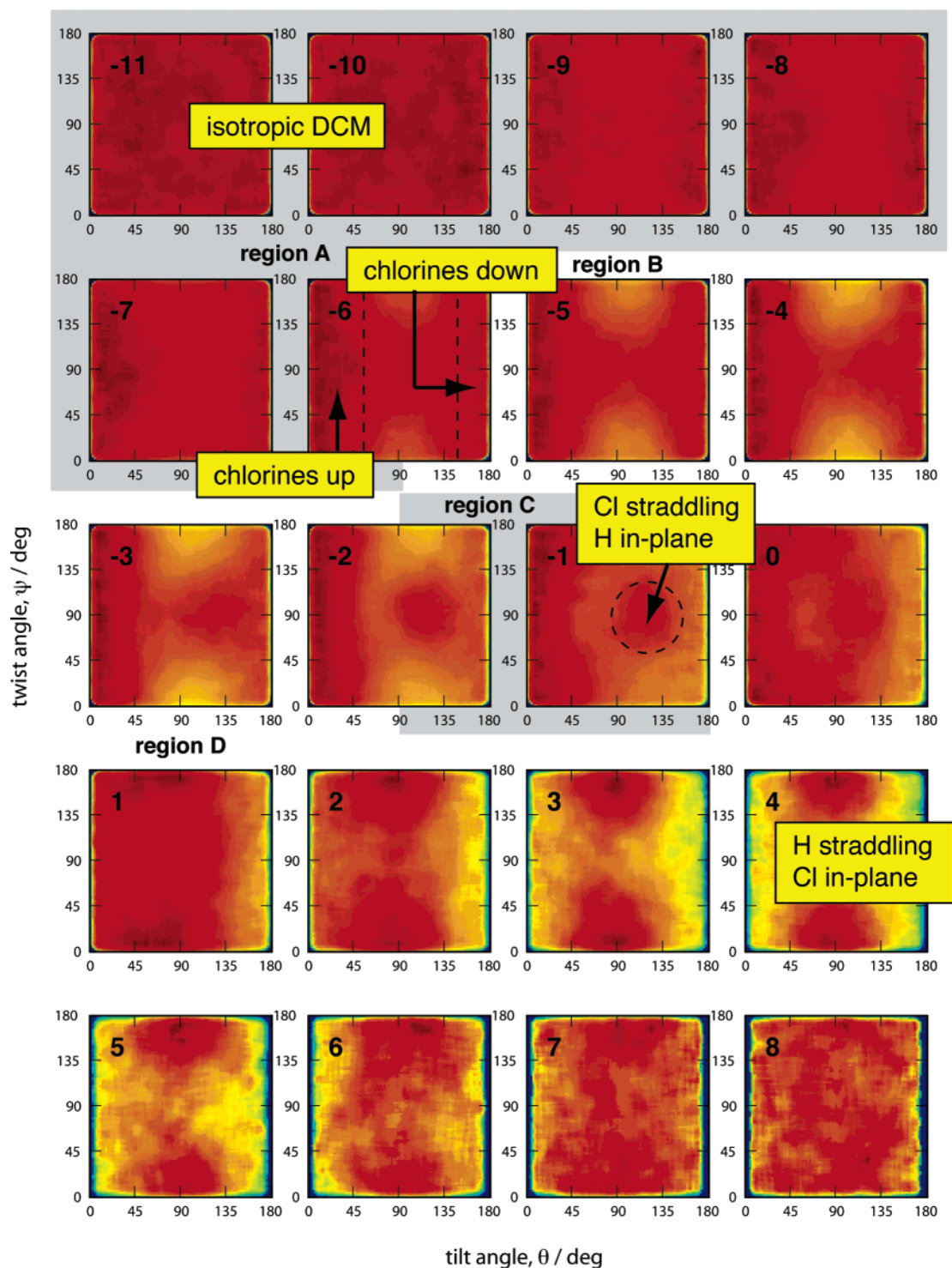


Figure 12. Snapshots of dichloromethane orientation at the dichloromethane–water interface. Blue indicates the smallest population; red indicates the largest population. Bold inset numbers indicate distance (in angstroms) from the Gibbs dividing surface. Negative values are on the bulk organic side; positive values are on the bulk water side. Shaded gray background is used to distinguish regions A–D, classified according to the order parameters in Figure 9.

such a sizable out-of-plane dipole moment in this region from primarily in-plane water molecules. In the case of the chloroform–water interface, this subset of the water population actually dominates the out-of-plane response of all of the water molecules (Figure 8). For the DCM–water interface, the same features are observed, but the out-of-plane dipole moment on the organic side of the interface (with opposite polarity, Figure 14) is larger. These important observations are possible as a result of our large and lengthy simulations and the clarity of the histogram images imparted by the median filtering.

Considering all of these structural features for both the water and organic molecules allows us to evaluate the net out-of-plane dipole moment across the interface. Results of the chloroform–water interface are summarized in Figure 15a, illustrating that a net dipole moment perpendicular to the interface is observed from $z = -7 \text{ \AA}$ in the chloroform to $z = +7 \text{ \AA}$ in the bulk water phase. The interfacial dipole is oriented such that it would attract negative ions, such as hydroxide, from the bulk water phase to create a negatively charged interface, in agreement with what is generally observed for water–hydrophobic liquid or

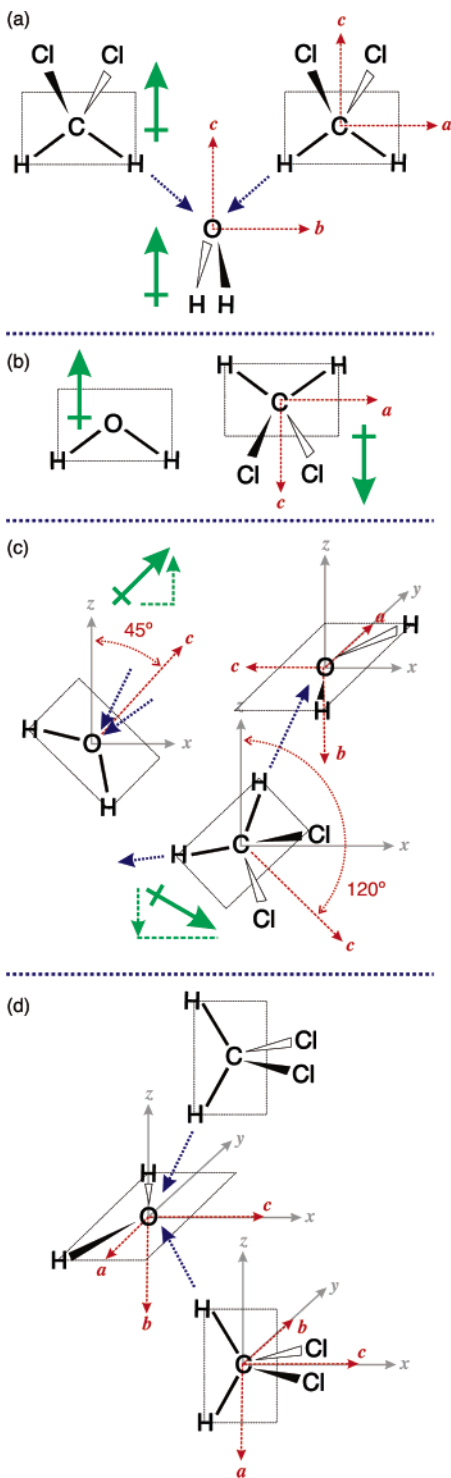


Figure 13. Predominant orientations of DCM and water molecules (a,b) furthest into the organic liquid (regions A and B), (c) close to the Gibbs surface in region C, and (d) furthest into the bulk water in region D. Dashed blue arrows indicate hydrogen bonds between water and DCM; green arrows show the direction of the permanent dipole moments.

solid interfaces.^{38,58} Our results predict a more complicated dipole pattern for the water–DCM interface as illustrated in Figure 15b. First we observe a much smaller dipole moment in the same direction on the bulk water side of the DCM–water interface, from $z = 2 - 7 \text{ \AA}$, likely attracting fewer anions from bulk water. From our structural results, we can see the origin of this dipole moment in the large population of water molecules on the DCM side of the GS with their oxygens pointing toward

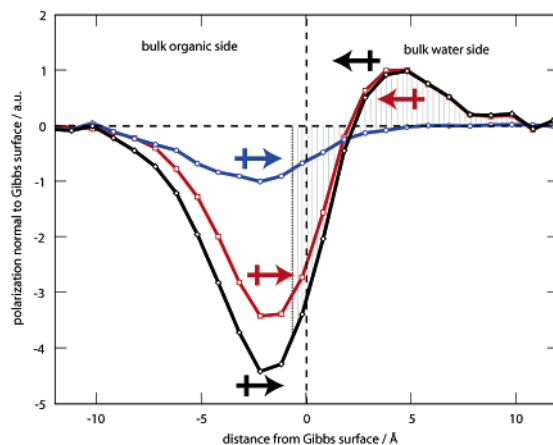


Figure 14. The z component of the net dipole moment for 1 \AA slabs through the dichloromethane–water interface. Contributions from water molecules are shown in red, dichloromethane in blue, total out-of-plane dipole moment in black. The sign of the polarization indicates the direction of the net dipole moment, depicted with arrows. The hatched area under the total dipole moment curve corresponds to regions with significant water density.

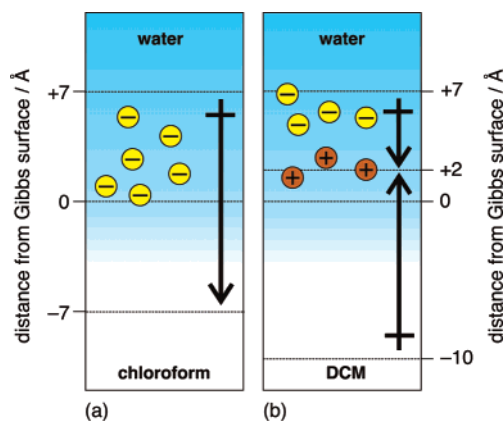


Figure 15. (a) For the chloroform–water interface, there is a net out-of-plane dipole moment oriented such that hydroxide ions from the bulk water phase would be attracted to the interface. (b) For the dichloromethane–water interface, there is a net dipole moment over a larger region, but it is not unidirectional. Negative ions would be attracted to the topmost layer, closest to the bulk water; positive ions would accumulate in a narrow region close to the Gibbs surface.

the bulk water phase. Considering that the adjacent layer of water molecules closer to the interface has a straddling orientation, it is reasonable to suspect that an oxygen-up orientation would maximize the number of water–water hydrogen bonds. However, this far into the bulk organic phase, it would normally be difficult for water molecules to exhibit any strong orientational preference. We suspect that this water molecule orientation is stabilized by DCM as a result of its own large permanent dipole moment. Below this region, extending to a depth of $z = -10 \text{ \AA}$ in the DCM, there is a large out-of-plane dipole moment in the opposite direction. As a result, there is a small region (a few angstroms wide) centered at the Gibbs surface that is likely to attract cations from the bulk water phase. It would be interesting to compare these predictions with experimental measurements of the interfacial potential. However, although liquid-surface potentials may readily be measured,⁵⁹ the difference between internal (Galvani) potentials for liquid–liquid interfaces cannot be measured directly.⁶⁰

It is important to note that a more rigorous calculation of the surface polarization must take into account contributions from not only the permanent dipole moments of the molecules but

also the induced dipole moments and local field effects. This would necessitate more sophisticated methods of simulation such as quantum or mixed quantum-classical molecular dynamics and the incorporation of flexible water and organic geometries and force fields. Nevertheless, the component of the permanent dipole moment normal to the interface is an important and significant contributor to the interfacial polarization. Our results indicate that in both the chloroform–water and DCM–water systems the balance between the organic and water dipole moments to create the net dipole moment in each layer is not a subtle one: orientations of the molecules create strongly enhancing dipole contributions in many regions of the interface. It is anticipated that, although future simulations will be able to measure these effects in a more quantitative manner, the overall trends would remain the same.

5. Conclusions

Equilibrium molecular dynamics simulations have been used to investigate the structure of chloroform–water and dichloromethane–water interfaces. A detailed study of orientation of water and organic molecules has been performed as a function of distance from the Gibbs surface. The results have been presented in terms of tilt and twist angle order parameters and orientation histograms. In these two interfacial systems, both water and organic molecules may reorient to minimize the surface free energy. It appears that the minimum energy structure is a balance between dipole compensation and hydrogen-bonding geometry optimization. In cases where creating hydrogen bonds is more energetically favorable, a significant net dipole moment perpendicular to the plane of the interface may exist. For the chloroform–water system, this net dipole is oriented such that a slight positive charge occurs on the bulk water side of the interface. This may be responsible for the purported enhancement of hydroxide ions at water–hydrophobic interfaces. However, when the same analysis is applied to the dichloromethane–water system, a more complex field pattern is observed with a much smaller dipole moment on the bulk water side of the interface. We aspire that our results will lead to a better understanding of the adsorption of large and small electrolytes, biomolecules, and other surfactants at these interfaces.

Acknowledgment. We thank the Department of Energy, Basic Energy Sciences (DEFG02-96ER45557) for the financial support of this project. L.M. was supported by the NSF REU program.

References and Notes

- (1) Schnell, B.; Schurhammer, R.; Wipff, G. *J. Phys. Chem. B* **2004**, *108*, 2285–2294.
- (2) Schurhammer, R.; Engler, E.; Wipff, G. *J. Phys. Chem. B* **2001**, *105*, 10700–10708.
- (3) Muzet, N.; Engler, E.; Wipff, G. *J. Phys. Chem. B* **1998**, *102*, 10772–10788.
- (4) Miller, R.; Fainerman, V. B.; Makievski, A. V.; Krägel, J.; Grigoriev, D. O.; Kazakov, V. N.; Sinyachenko, O. V. *Adv. Colloid Interface Sci.* **2000**, *86*, 39–82.
- (5) Nichols, M. R.; Moss, M. A.; Reed, D. K.; Hoh, J. H.; Rosenberry, R. L. *Biochemistry* **2005**, *44*, 165–173.
- (6) Lu, G.; Chen, H.; Li, J. *Colloids Surf., A* **2003**, *215*, 25–32.
- (7) Urzúa, M. D.; Ros, H. E. *Polym. Int.* **2003**, *52*, 783–789.
- (8) Liu, B.; Qian, D. J.; Huang, H.-X.; Wakayama, T.; Hara, S.; Huang, W.; Nakamura, C.; Miyake, J. *Langmuir* **2005**, *21*, 5079–5084.
- (9) Wang, L.; Zhu, G.; Wang, P.; Zhang Newby, B.-m. *Biotechnol. Prog.* **2005**, *21*, 1321–1328.
- (10) Zhu, G.; Wang, P. *J. Am. Chem. Soc.* **2004**, *126*, 11132–11133.
- (11) Speakman, J. *J. Chem. Soc.* **1933**, 1440.
- (12) Ikeda, T.; Ozaki, T. *Bull. Chem. Soc. Jpn.* **1950**, *23*, 43–45.
- (13) Aoki, M.; Ohashi, Y.; Masuda, S. *Surf. Sci.* **2003**, *532*–535, 137–141.
- (14) Picaud, S.; Hoang, P. N. M. *Phys. Chem. Chem. Phys.* **2004**, *6*, 1970–1974.
- (15) Holmes, N. S.; Sodeau, J. R. *J. Phys. Chem. A* **1999**, *103*, 4673–4679.
- (16) Boury, F.; Ivanova, T.; Panaïotov, I.; Proust, J. E.; Bois, A.; Richou, J. *J. Colloid Interface Sci.* **1995**, *169*, 380–392.
- (17) Balashev, K.; Bois, A.; Proust, J. E.; Ivanova, T.; Petkov, I.; Masuda, S.; Panaïotov, I. *Langmuir* **1997**, *13*, 5362–5367.
- (18) Malzert, A.; Boury, F.; Saulnier, P.; Ivanova, T.; Panaïotov, I.; Benot, J. P.; Proust, J. E. *J. Colloid Interface Sci.* **2003**, *259*, 398–407.
- (19) Babak, V. G.; Boury, F. *Colloids Surf., A* **2004**, *243*, 33–42.
- (20) Wan, C.; Chen, Y. H.; Wei, R. *Environ. Toxicol. Chem.* **1999**, *18*, 1091–1096.
- (21) Nagy, P. I.; Takács-Novák, K. *J. Am. Chem. Soc.* **2000**, *122*, 6583–6593.
- (22) Berthod, A.; Georges, J. *J. Colloid Interface Sci.* **1985**, *106*, 194–202.
- (23) Boury, F.; Olivier, E.; Proust, J. E.; Benot, J. P. *J. Colloid Interface Sci.* **1994**, *163*, 37–48.
- (24) Saulnier, P.; Boury, F.; Malzert, A.; Heurtault, B.; Ivanova, T.; Cagna, A.; Panaïotov, I.; Proust, J. E. *Langmuir* **2001**, *17*, 8104–8111.
- (25) Sah, H. *J. Controlled Release* **1999**, *58*, 143–151.
- (26) van de Weert, M.; Hoehsteter, J.; Hennink, W. E.; Crommelin, D. J. A. *J. Controlled Release* **2000**, *68*, 351–359.
- (27) Pérez, C.; Griebenow, K. *J. Pharm. Pharmacol.* **2001**, *53*, 1217–1226.
- (28) Malzert, A.; Boury, F.; Saulnier, P.; Benot, J. P.; Proust, J. E. *Langmuir* **2002**, *18*, 10248–10254.
- (29) Sah, H.; Bahl, Y. *J. Controlled Release* **2005**, *106*, 51–61.
- (30) Bahramian, A.; Danesh, A. *Fluid Phase Equilib.* **2004**, *221*, 197–205.
- (31) Dang, L. X. *J. Chem. Phys.* **1999**, *110*, 10113–10122.
- (32) Adam, N. K. *The Physics and Chemistry of Surfaces*; Oxford University Press: London, 1941.
- (33) Bikerman, J. J. *Surface Chemistry: Theory and Applications*; Academic Press: New York, 1958.
- (34) Chattoraj, D. K.; Birdi, K. S. *Adsorption and the Gibbs Surface Excess*; Plenum: New York, 1984.
- (35) Jungwirth, P.; Tobias, D. J. *J. Phys. Chem. B* **2002**, *106*, 6361–6373.
- (36) Mucha, M.; Frigato, T.; Levering, L. M.; Allen, H. C.; Tobias, D. J.; Dang, L. X.; Jungwirth, P. *J. Phys. Chem. B* **2005**, *109*, 7617–7623.
- (37) Kreuzer, H. J.; Wang, R. L. C.; Grunze, M. *J. Am. Chem. Soc.* **2003**, *125*, 8384–8389.
- (38) Zangi, R.; Engberts, J. B. F. N. *J. Am. Chem. Soc.* **2005**, *127*, 2272–2276.
- (39) Case, D. A. et al. *Amber 7*; University of California: San Francisco, CA, 2002.
- (40) Chang, T.-M.; Dang, L. X. *J. Phys. Chem. B* **1997**, *101*, 10518–10526.
- (41) Dang, L. X. *J. Phys. Chem. B* **2001**, *105*, 804–809.
- (42) Jedlovsky, P.; Vincze, A.; Horvai, G. *J. Mol. Liq.* **2004**, *109*, 99–108.
- (43) Jedlovsky, P.; Vincze, Á.; Horvai, G. *Phys. Chem. Chem. Phys.* **2004**, *6*, 1874–1879.
- (44) Buffeteau, T.; Lagugné, Labarthe, F.; Sourisseau, C.; Kostromine, S.; Bieringer, T. *Macromolecules* **2004**, *37*, 2880–2889.
- (45) Straley, J. P. *Phys. Rev. A* **1974**, *10*, 1881–1887.
- (46) Photinos, D. J.; Bos, P. J.; Doane, J. W.; Neubert, M. E. *Phys. Rev. A* **1979**, *20*, 2203–2211.
- (47) Collings, P. J.; Photinos, D. J.; Bos, P. J.; Ukleja, P.; Doane, J. W. *Phys. Rev. Lett.* **1979**, *42*, 996–999.
- (48) Stone, D. C. *Can. J. Chem.* **1995**, *73*, 1573–1581.
- (49) Meyer-Arendt, J. R. *Two-Dimensional Digital Signal Processing*; Springer-Verlag: Secaucus, NJ, 1981; Vol. 2.
- (50) Morita, A.; Hynes, J. T. *Chem. Phys.* **2000**, *258*, 371–390.
- (51) Morita, A.; Hynes, J. T. *J. Phys. Chem. B* **2002**, *106*, 673–685.
- (52) Perry, A.; Ahlborn, H.; Space, B.; Moore, P. B. *J. Chem. Phys.* **2003**, *118*, 8411–8419.
- (53) DeVane, R.; Space, B.; Perry, A.; Neipert, C.; Ridley, C.; Keyes, T. *J. Chem. Phys.* **2004**, *121*, 3688–3701.
- (54) Chang, T.-M.; Dang, L. X. *J. Chem. Phys.* **1996**, *104*, 6772–6783.
- (55) Moreira, N. H.; Skaf, M. S. *Prog. Colloid Polym. Sci.* **2004**, *128*, 81–85.
- (56) Jedlovsky, P.; Vincze, A.; Horvai, G. *J. Chem. Phys.* **2002**, *117*, 2271–2280.
- (57) Jedlovsky, P.; Kereszturi, A.; Horvai, G. *Faraday Discuss.* **2005**, *129*, 35–46.
- (58) Schurhammer, R.; Wipff, G. *New J. Chem.* **1999**, *23*, 381–391.
- (59) Peterson, I. R. *Rev. Sci. Instrum.* **1999**, *70*, 3418–3424.
- (60) Markin, V. S.; Volkov, A. G. *Adv. Colloid Interface Sci.* **1990**, *31*, 111–152.